

Anticancer Bioactive Compound from Marine *Bacillus aquimaris* (KU318396) Induces Apoptosis in Lung (A549) Cancer Cells by Inhibition of Anti-Apoptotic Family Proteins

Nithin Unnikrishnan¹ , Arya Vijayan¹ , Keerthi Raghavan^{1,*} 

¹ School of Biosciences, Mahatma Gandhi University, Kottayam, Kerala, India

* Correspondence: keerthihalakattilraghavan@gmail.com;

Scopus Author ID 55929879800

Received: 20.08.2022; Accepted: 20.09.2022; Published: 17.11.2022

Abstract: The apoptotic potential of the secondary metabolites extracted from the marine *Bacillus aquimaris* sp was evaluated. The ethyl acetate extract was purified by silica gel column chromatography and preparative HPLC. The purified fraction was used for cytotoxicity assay and evaluation of apoptosis. Cell cycle analysis and apoptotic-related gene expression study were performed to confirm the apoptosis. Structure elucidation of the compound was done by LCMS/MS. A molecular docking study was performed by using anti-apoptotic proteins as target enzymes. The fraction-treated lung cancer cells exhibited characteristic morphological changes of apoptosis, and cell cycle analysis indicated that the fraction was very effective in G1 phase arrest. Further, the treated group exhibited the decreased expression of anti-apoptotic genes and activation of pro-apoptotic genes, besides overexpression of p53. The structure of the compound was revealed by LCMS/MS analysis. A molecular docking study of the compound showed significant binding interaction with anti-apoptotic proteins. The study concluded that this is the first report on the anticancer activity of a bioactive compound from *Bacillus aquimaris* sp (KU318396) against lung cancer. Moreover, the study also reports the purified novel compound induced apoptosis in lung (A549) cancer cells by inhibiting Bcl-2 and Bcl-XL.

Keywords: *Bacillus aquimaris*; secondary metabolites; cytotoxicity; lung cancer, apoptosis; molecular docking.

© 2022 by the authors. This article is an open-access article distributed under the terms and conditions of the Creative Commons Attribution (CC BY) license (<https://creativecommons.org/licenses/by/4.0/>).

1. Introduction

Cancer is a disease in which a person's cells can proliferate and spread uncontrollably to other parts of the body because of genetic or epigenetic abnormalities [1]. Lung cancer is the most frequently seen cancer and is also reported as the foremost cause of cancer-related death [2]. Non-small cell lung cancer (NSCLC) was found to be insensitive to the treatments and constitutes about 85% of all lung cancer, including squamous cell carcinoma, adenocarcinoma, Etc [3]. Although chemotherapeutic interventions have been used extensively to treat lung cancer, the emergence of drug resistance and adverse effects make it challenging to ensure the therapy's success [4].

Apoptosis is a programmed cell death process that contributes to the eradication of unwanted cells to sustain the balance between cell survival and cell death [5]. Apoptosis is a

highly selective process and is important in both normal and pathological conditions [6]. Secondary metabolites derived from marine sources induce cell death in a number of ways to counteract the anti-apoptotic characteristics of cancer cells [7]. Apoptotic induction and cell cycle arrest are recognized as the imperative strategies to kill cancer cells [8]. Many anticancer bioactive metabolites were discovered in marine microorganisms, and some are currently undergoing various stages of clinical testing [9].

According to recent investigations, marine microorganisms could be the source of novel bioactive secondary metabolites with anti-proliferative and apoptotic effects [10]. Marine *Bacillus sp* represents a rich source of structurally diversified classes of metabolites, including lipopeptides, cyclic peptides, polypeptides, macrolactones, unsaturated fats, polyketides, and lipoamides [11]. These metabolites of marine isolates are produced as part of complex biosynthetic pathways and have a wide variety of therapeutic functions [12]. Usually, organic solvents like chloroform and ethyl acetate are used to extract the secondary metabolites produced by the microorganisms [13].

Bacillus aquimaris, a moderately halophilic bacteria also found to be organic solvent tolerant and synthesize commercially important enzymes [14]. The antagonistic activities of *Bacillus aquimaris* have been evaluated [14]; its anticancer properties have not been studied so far. Therefore, in the present study, for the first time, we report the purification, structural identification, and evaluation of the anticancer potential of a novel biomolecule produced by marine *Bacillus aquimaris* MB3.

2. Materials and Methods

2.1. Identification of marine bacteria.

The bacteria isolated from marine sediments of Fort Cochin, Kerala, India (9.9658° N, 76.2421° E) was used. The molecular identification of marine bacteria designated as MB3 was carried out by 16S rDNA gene sequencing [15]

2.2. Extraction of bioactive compounds.

The bacteria have grown large scale in Zobell's marine broth 2216 (Himedia) and incubated on a rotary shaker (120 rpm) at 37°C for five days. The bioactive compound from the fermented broth was extracted twice with ethyl acetate (obtained after sequential extraction followed by hexane and chloroform). The organic layer was removed and concentrated in a rotary evaporator [15]. The dried ethyl acetate extract was then subjected to cytotoxicity studies.

2.3. Cell lines and cell culture conditions.

Lung (A549) cancer cells and L929 (Fibroblast) normal cells purchased from National Centre for Cell Sciences (NCCS), Pune, India, and maintained in Dulbecco's modified Eagles medium (Sigma Aldrich, USA) were used. The cell line was cultured in DMEM supplemented with 10% FBS, L-glutamine, sodium bicarbonate (Merck, Germany), and an antibiotic solution containing: Penicillin (100U/ml), Streptomycin (100µg/ml), and Amphotericin B (2.5µg/ml). Cultured cell lines were kept at 37°C in a humidified 5% CO₂ incubator (NBS Eppendorf, Germany).

2.3.1. Cytotoxicity assay.
Cytotoxicity of the ethyl acetate extract was measured by 3-(4, 5-dimethylthiazol-2-yl)-2,5-diphenyl tetrazolium bromide (MTT) reduction assay [16]. Lung cancer (A549) cells and normal fibroblast (L929) cells were seeded at a density of 5x10⁴ cells and incubated for 24h.

various concentrations of ethyl acetate extract (6.25, 12.50, 25.00, 50.00, and 100.00 µg/mL) were treated with the (A549) cells and dissolved in 0.1% dimethyl sulphoxide (DMSO) for 24 h at 37°C in 5% CO₂ incubator. After 24 h, 20 µL of 5mg/mL MTT (pH: 7.4) solution was added to all the wells and incubated for 3 hours in a 5% CO₂ incubator. The medium was aspirated and then added with DMSO to dissolve the purple formazan crystals. The 540 nm wavelength was applied to measure the absorbance values (Elisa Reader- Erba, Germany). The entire plate was observed by an inverted phase contrast microscope (Olympus CKX41 with Optika Pro5 CCD camera). The percentage inhibition of growth was calculated.

2.4. Purification of the ethyl acetate extract.

The ethyl acetate extract was used for bioassay-guided fractionation by using a silica gel (80- 120 mesh) column and eluted using chloroform: methanol of different gradients and the flow rate of the column was adjusted to be 0.5 mL/minute[17]. Twelve fractions were collected and selected for cytotoxicity assay. The fraction which showed significant cytotoxicity was selected and again purified by preparative HPLC, using Waters 2695 HPLC, photodiode array detector (PDA), and Column puresil 5µm C18 4.6x150 mm. The volume injected was 100 µL under the conditions of average pressure of 1.267 psi, and the flow rate was 1 mL/min, where the mobile phase was 0-45% methanol: water and the time period was 25 min [18]. Cytotoxicity of bioactive fractions, HPLC fraction, and reference standard (Vincristine sulfate) was determined by MTT assay as described in section 2.3.1.

2.5. Morphological observation.

2.5.1. Live cell imaging.

Cancer cells (5×10^4 cells) were seeded and treated with the IC₅₀ concentration of HPLC fraction for 24 h. After incubation, the cells were checked for morphological irregularities using an inverted phase contrast microscope.

2.5.2. Acridine orange/ethidium bromide staining.

DNA-binding dyes Acridine Orange (AO) and Ethidium Bromide (EB) (Sigma, USA) were used for the observation of morphologically abnormal apoptotic cells [19]. The cells were treated with the IC₅₀ concentration of HPLC bioactive fraction for 24 h and washed with cold PBS (pH 7.4). The dyes AO (100 g/mL) and EB (100 g/mL) were combined and stained the cells at room temperature for 10min. The stained cells were again washed with PBS and visualized under a fluorescence microscope using a blue filter (Olympus CKX41 with Optika Pro5 camera).

2.6. Gene expression analysis

2.6.1. Isolation of total RNA (Trizol method).

The lung cancer (A549) cells (5×10^4 cells) were treated with the IC₅₀ concentration of the HPLC fraction and incubated for 24 hours in a CO₂ incubator. Untreated control cells were also incubated. After incubation, the media was removed, 200 µL of Trizol reagent was added, and incubated for 5 minutes. To this, 200 µL of chloroform was added, homogenized vigorously for 15 seconds, and incubated for 3 minutes at room temperature, followed by centrifugation

at 12000 rpm for 10 minutes at 4°C. To the aqueous layer, 500µL of 100% isopropanol was added and incubated for 10 min at room temperature, followed by centrifugation at 12000 rpm for 10 min at 4°C. After discarding the supernatant, the pellet obtained was washed with 200µL of 75% ethanol and centrifuged at 12000rpm for 5 minutes at 4°C. Finally, the RNA pellet obtained was dried and suspended in TE buffer [20].

2.6.2. Reverse transcriptase PCR Analysis.

Thermo scientific's Verso cDNA synthesis kit (AB-1453/A) was used for the cDNA synthesis. About 4µL of 5X cDNA synthesis buffers, 2µL of dNTP mix, 1µL of anchored oligodT, 1µL of RT Enhancer, 1µL of Verso Enzyme Mix, and 5µL of RNA template (1ng of total RNA) were added to an RNase free tube. Then the total reaction volume was made up to 20 µL with the addition of sterile distilled water. The solution was mixed by pipetting gently up and down. The thermal cycler (Eppendorf Master Cycler) was programmed to undergo cDNA synthesis. The following cycling conditions were employed: -30 min at 42°C for cDNA synthesis and 2 min at 95°C for inactivation [21].

The primers anti-apoptotic genes Bcl-2 (F: 5'-CCTGTGGATGACTGAGTA-3'R: GAGACAGCCAGGAGAAATCA-3') and Bcl-XL (F: 5'-CTGGTGGTTGACTTTCTCTC-3' R 5'-GAGTTCATTCACCTGTTT-3'). The pro-apoptotic genes Bax (F: 5'-CCACCATGAGCGCTGCTCA-3' R: 5'-GCAGGGGAGGGAGAGATG-3'). Tumor suppressor gene p53 (F: 5'-TCCCCCGAGAGGTCTTTT-3' R: 5'-CGGCCCCAGTTGAAGTTG-3'), and the housekeeping gene β-actin (*ACTB*) was used to normalize the gene expression values (F: 5'-GAGACCTTCAACCCCCAGCC-3' R: 5'-AGACGCAGGATGGCATGGG-3'). The amplification was done using a Thermo scientific amplification kit. The following components were added for each 50 µL reaction: 25 µL of PCR Master Mix (2X), 2 µL of Forward primer (0.1-1.0 µM), 2 µL of Reverse primer (0.1-1.0 µM), and 5 µL of Template DNA (10 pg- 1 µg). The components were made up to 50 µL with sterile distilled water. Initial denaturation at 95°C for 3 min, followed by denaturation at 95°C for the 30s, annealing at 52°C for 30s, and extension at 72°C for 1 minute, which was repeated for 35 cycles and the final extension at 72°C for 5 min. After the amplification, the stained gel was visualized using a gel documentation system (E gel imager, Invitrogen).

2.7. Cell cycle analysis.

Cell cycle analysis was performed by flow cytometric measurements of the DNA content of the cells by using Muse™ Cell Cycle Assay Kit (Millipore). The lung cancer (A547) cells (5×10^4 cells ml⁻¹) were seeded and treated with the IC₅₀ concentration of HPLC fraction for 24 h at 37°C. The treated cells were centrifuged at 3000 rpm for 5 min, washed with PBS, and fixed in 70% ethanol overnight at 4°C. After the incubation, the samples were centrifuged at 3000 rpm for 5 minutes at room temperature. The pellet was taken and stained with 20µg/ml propidium iodide, 100µg/ml RNase A, and 1% Triton X-100 in PBS for 30 min under the dark. The percentage of accumulated cells present in different phases of the cell cycle was analyzed in Flow Cytometer (Muse Cell Analyzer Millipore Germany) [22].

2.8. Characterization of bioactive metabolite in HPLC fraction.

To detect the presence of compounds, the HPLC fraction was filtered through a 0.22-µm membrane filter and subjected to LC-MS/MS analysis using Acquity H-Class (Waters)

ultra-performance liquid chromatography with BEH C18 column (50 mm× 2.1 mm×1.7 μm) and a Xevo G2 (Waters) quadrupole time of flight (Q-TOF) Mass spectrometer. The mobile phase was methanol at a flow rate of 0.2 mL min⁻¹. The electrospray ionization was used in positive mode to produce mass spectra with a scan range from 50 to 600, and the scan time was 6 min. The source and desolvation temperatures were 135°C and 350°C, respectively, and the capillary voltage was 4.50 kV.

2.9. Molecular docking.

Molecular docking studies were performed to determine the appropriate binding orientations and conformations of the isolated compound with apoptotic regulatory enzymes (Bcl-2, Bcl-XL) by using AutoDock 4.0. The molecular structure of the purified compound was downloaded from the ChemSpider database (<https://www.chemspider.com>). The ligand was then converted to .pdb format using Open Babel software (<http://openbabel.org>). The 3D structure coordinates of target enzymes (Bcl-2 and Bcl-XL) were retrieved from the protein data bank repository (<http://www.rcsb.org>) with PDB id's 4AQ3 and 2YQ6, respectively. The heteroatoms, unwanted connectors, and water molecules were removed from the protein structure and underwent optimization and energy minimization using a program implemented in Swiss PDB Viewer(<http://spdbv.vital-it.ch/disclaim.html>) [23].

2.9.1. Molecular docking simulation.

Molecular docking of the target protein and the ligand were performed by using AutoDock 4.0 software. The automatic settings default parameters were used to run the docking simulation. The ligand was manually docked into functional sites individually to the protein, and the docking energy was monitored to attain a minimum value. In the protein, polar hydrogen atoms were merged, and the total Kollman charge was added. Lamarckian Genetic Algorithm (LGA) was employed for the automated docking of proteins with ligands [24]. The ligands' torsion bonds and side chains were allowed to rotate freely while the target was kept rigid. Polar hydrogen atoms were added to targets, while Gasteiger charges were computed. LGA was implemented by creating an initial population of 150 individuals, applying random torsions to each of the 150 individuals, and performing a maximum of 500000 energy evaluations in each docking run. The further step is preparing PDBQT format files for both target and compound and creating Grid and Docking Parameter files (.gpf and .dpf) using AutoDock 4.2. During docking, a grid of 60x60x60 points in x, y, and z directions was built with a grid spacing of 0.375 Å using the AutoGrid component of the software. At least ten such runs were performed for all ligands, and the best conformation with the lowest docked energy was chosen. The final step is to perform molecular docking using Cygwin (<http://www.cygwin.com>), and finally, the results are analyzed. The docked structure's best binding modes were visualized using UCSF Chimera software.

2.9.2 ADMET analysis.

The compounds with good binding energies obtained from the docking studies were further selected to analyze their ADMET (absorption, distribution, metabolism, excretion, and toxicity) properties [25]. The two-dimensional structure of the compound was drawn in the ChemSketch version (www.acdlabs.com/chemsketch), and the mol file of the compound was translated into SMILES. Then the online software Molsoft tool (<https://molsoft.com/mprop>)

was used to generate *in silico* pharmacokinetics parameters of the compound to estimate their drug-likeness properties.

2.10. Statistical analysis.

Statistical analyses were done using GraphPad Prism 5.0 (GraphPad Software, Inc., San Diego, CA). The comparison of treatment groups and controls was made through a one-way analysis of variance (ANOVA) and Tukey's multiple-comparison posttest. Results were designated significant when the P-value (P) < 0.05: * = P < 0.05, ** = P < 0.01, *** = P < 0.001, **** = P < 0.0001, ns = non-significant. The outcomes are expressed as mean ± S.D.

3. Results and Discussion

3.1. Identification of marine bacteria.

Molecular identification of the bacteria designated as MB3 was done by sequencing the 16S rDNA gene. Based on the homology of the 16S rDNA sequence, the strain showed 99% similarity with *Bacillus aquimaris* sp. The sequence data were submitted to NCBI under the accession number (KU318396).

3.2. Extraction of bioactive compounds.

The Bacteria were grown on a large scale under suitable conditions, and the bioactive compounds produced in the culture broth were extracted using ethyl acetate. The dry weight of the extract was calculated as 0.68g and used for further studies.

3.3. Cytotoxicity assay.

Invitro inhibitory activity of ethyl acetate extract was evaluated by MTT assay. The cytotoxicity assay inferred that the ethyl acetate extract inhibited the Lung (A549) cancer cell lines in a dose-dependent manner, and the IC₅₀ concentration was found to be 69.56±2.18µg/mL at 24-hour exposure, as shown in Figure 3. This extract was used for further purification.

3.4. Purification of ethyl acetate extract.

The purification of ethyl acetate extract was performed by silica gel column chromatography, and twelve fractions were obtained.

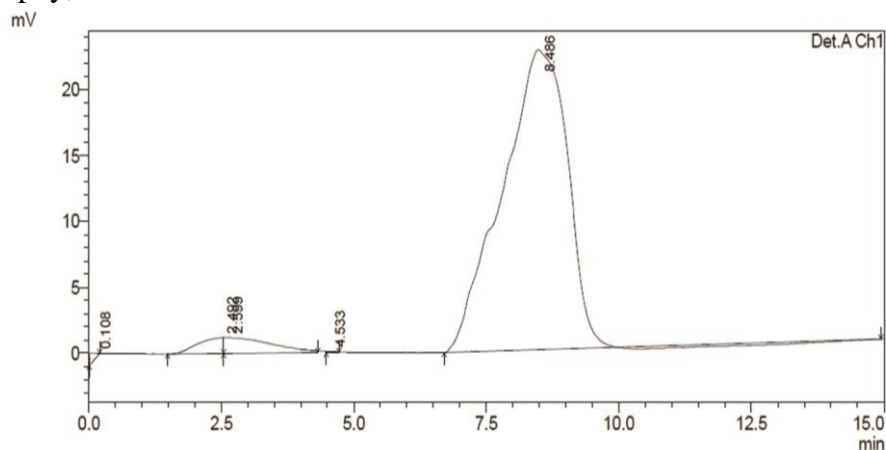


Figure 1. HPLC chromatogram of bioactive fraction F6.

The fractions were then subjected to cytotoxicity assay to get a bioactive fraction. The sixth fraction (chloroform: methanol 50:50) showed significant cytotoxicity with an IC₅₀ concentration of 50.54±1.80µg/mL and hence was selected for further purification by HPLC. The bioactive fraction F6 showed one prominent peak at retention time (Rt) 8.486. The chromatogram is shown in Figure 1.

The collected HPLC fraction showed an IC₅₀ value of 26.40 ± 0.76µg/mL, which is comparable with the IC₅₀ concentration of Vincristine sulfate 20.07 ± 0.15µg/mL shown in Figure 2.

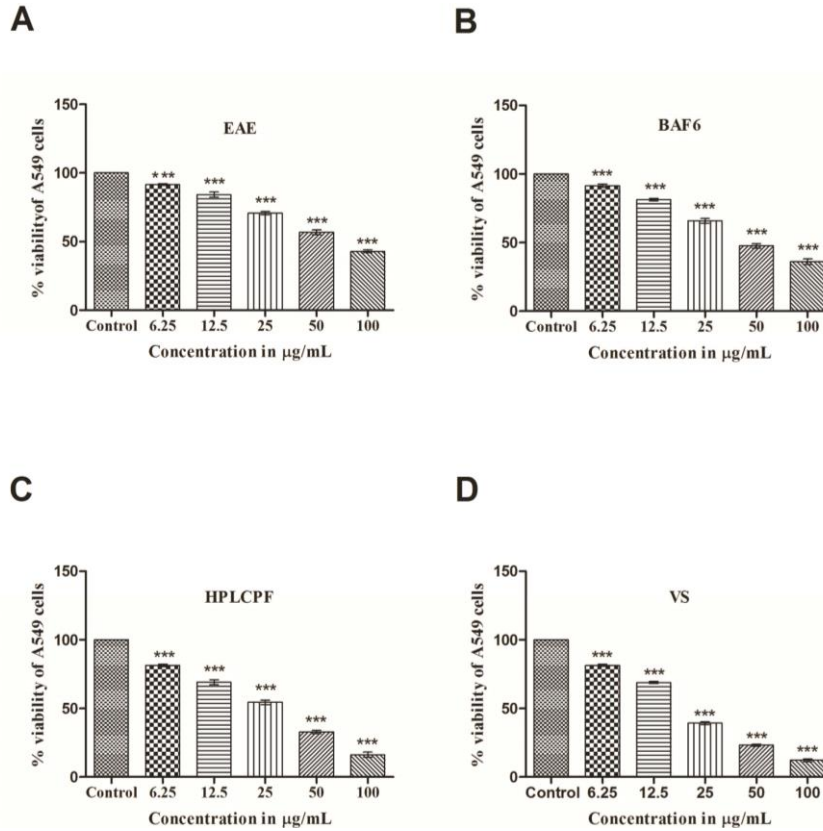


Figure 2. Dose-dependent inhibition; (A) Ethyl Acetate Extract (EAE); (B) Bioactive Fraction 6 (BAF6); (C) HPLC Purified Fraction (HPLCPF); (D) Vincristine Sulfate (VS) treated lung (A549) cancer cells. The level of significance was * =P < 0.05, ***= P < 0.001.

The study also revealed that the HPLCPF showed significant toxicity toward lung (A549) cells. The HPLCPF-treated cells showed morphological aberrations of cytotoxicity, such as cell size reduction, cell shrinkage, and cleavage of the cell membrane, which was comparable with the reference standard treated cells.

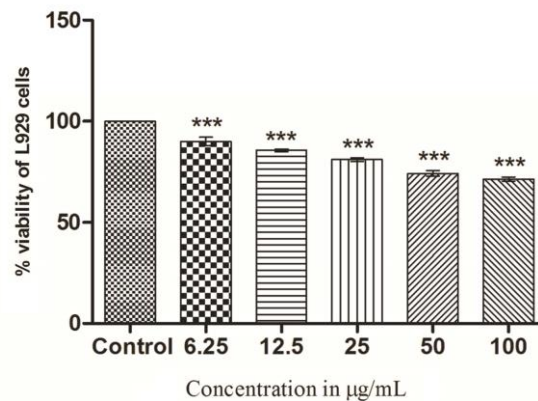


Figure 3. Cytotoxic effect of HPLC pure fraction on normal L929 cells.

The HPLCPF showed no toxic effects on the viability of L929 (Fibroblast) cells, as shown in Figure 3. Earlier reports revealed that the bioactive compound abbreviated as "PPDHMP" isolated from *Staphylococcus sp* showed anticancer activity against lung cancer (A549) cells [26].

3.5. Morphological observation.

3.5.1. Live cell imaging.

The IC₅₀ concentration of HPLCPF-treated A549 cells showed significant cytotoxicity, such as the cells becoming rounder and shrunken, and more than 50 % of cells showed membrane blebbing. The results are shown in Figure 4A.

3.5.2. AO/ EB staining.

Acridine orange (AO) and ethidium bromide (EB) dual staining were performed to determine the morphological changes of the treated cells due to apoptosis. In this study, A549 cells were treated with IC₅₀ concentration of HPLCPF, and untreated cells were maintained as control. The results indicated that untreated cells appeared green because the cell membrane was intact. The treated cells appeared red because the ethidium bromide penetrated the nucleus of dead cells and appeared red, demonstrating the apoptotic model of cell death. The results are shown in Figure 4B. The same results trend was observed when the 2,4- diacetylphloroglucinol (DAPG) was isolated from *Pseudomonas aeruginosa* strain-treated lung cancer cells [21]. The morphological and biochemical aberrations of the treated cells were observed due to the apoptotic induction, and it was the efficient approach in cancer treatment [27]

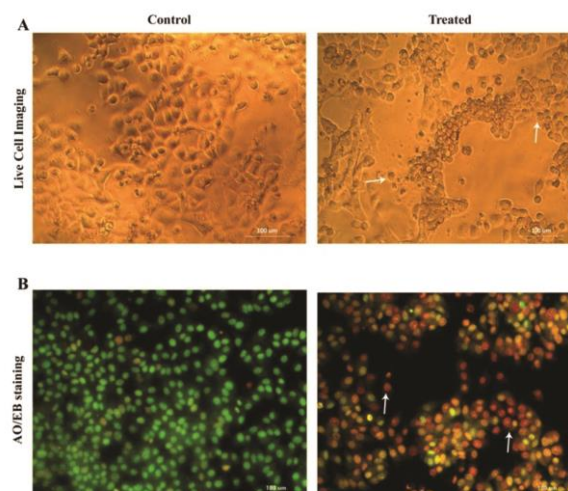


Figure 4. Morphological observation; (A) Live cell imaging of A549 control cells and treated with IC₅₀ concentration of HPLCPF: - cell shrinkage and cell membrane blebbing; (B) Fluorescent imaging after AO/EB double staining, control: viable cells appeared as green with intact nuclei, and IC₅₀ treated cells appeared as the early apoptotic (green-orange with condensed nuclear cells) and late apoptotic (fragmented red cells).

3.6. Gene expression studies.

Further, to understand the mechanism of apoptotic potential, the expression of significant regulators of apoptosis upon treatment with HPLCPF was noted. The treated sample showed increased expression of pro-apoptotic gene Bax and overexpression of tumor suppressor gene p53. From the results, it would be clear that the correlated expression of the

Bax and p53 genes effectively activates the apoptotic mechanism. The decreased expression of anti-apoptotic genes such as Bcl-2 and Bcl-XL was also revealed. Suppressing the Bcl-2 and Bcl-XL genes was a significant way of apoptosis. The results are shown in Figure 5. The initiation of apoptosis depends upon the balance between pro-apoptotic and anti-apoptotic proteins [28]. The early reports disclosed that the down-regulation of anti-apoptotic Bcl-2 family proteins was observed upon treatment with a novel anticancer metabolite from *Staphylococcus sp* against lung cancer cells [26]. The activated Bcl-2 pro-apoptotic proteins (Bax and Bak) increased the outer membrane permeability of mitochondria, facilitating the release of apoptogenic factors into the cytosol [29]. The Bax expression in the cancer cells increased significantly upon the treatment of DAPG. The increased expression of p53 regulates the significant genes that further lead to apoptosis and cell cycle arrest [21].

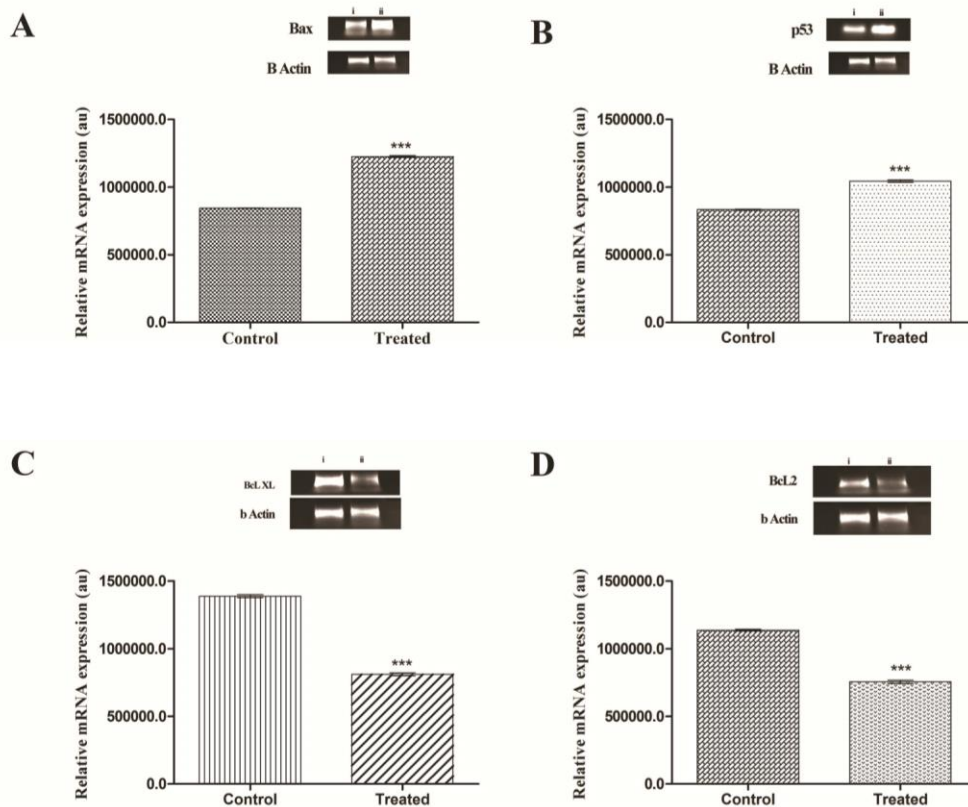


Figure 5. The relative mRNA expression; (A) Bax; (B) p53; (C) Bcl-XL; (D) Bcl-2 were analyzed by reverse transcriptase PCR (RT-PCR); β actin was used as internal loading control; i= control; ii= treated. The level of significance was*** $p < 0.001$.

3.7. Cell cycle analysis.

The lung cancer (A549) cells were treated with IC_{50} concentration of HPLCPF and stained with propidium iodide to determine the proportion of cells undergoing cell death or apoptosis by flow cytometry. These studies revealed the cell population distribution across various cell cycle phases, such as G0/G1, S, and G2/M. The untreated sample showed various proportions of cells, such as the G0/G1 phase showed 84.4% cells, the S phase consisting of 8.8% cells, and 4.5% cells in the G2M phase. The DNA content of the untreated cells is shown in Figure 6A.

The HPLCPF-treated A549 cells showed a decreased concentration of DNA in the S phase region (1.4%), and the results indicated the cell death and accumulation of cells in the G0/G1 phase (89.8%). Based on observation, the HPLCPF-treated cells showed G0/G1 phase

arrest and cell death in cancer cells shown in Figure 6B. The capability to initiate cell cycle arrest in cancer cells is a vital characteristic of a probable anticancer agent [30]. Our research revealed that treating cancer cells with HPLC fraction arrested major cells at the G1 phase of the cell cycle and found a low level of DNA content at the S phase. In addition, early reports disclosed that the anticancer bioactive compound produced by *Staphylococcus* sp arrests the cell cycle at the G1 phase and induces apoptosis [26].

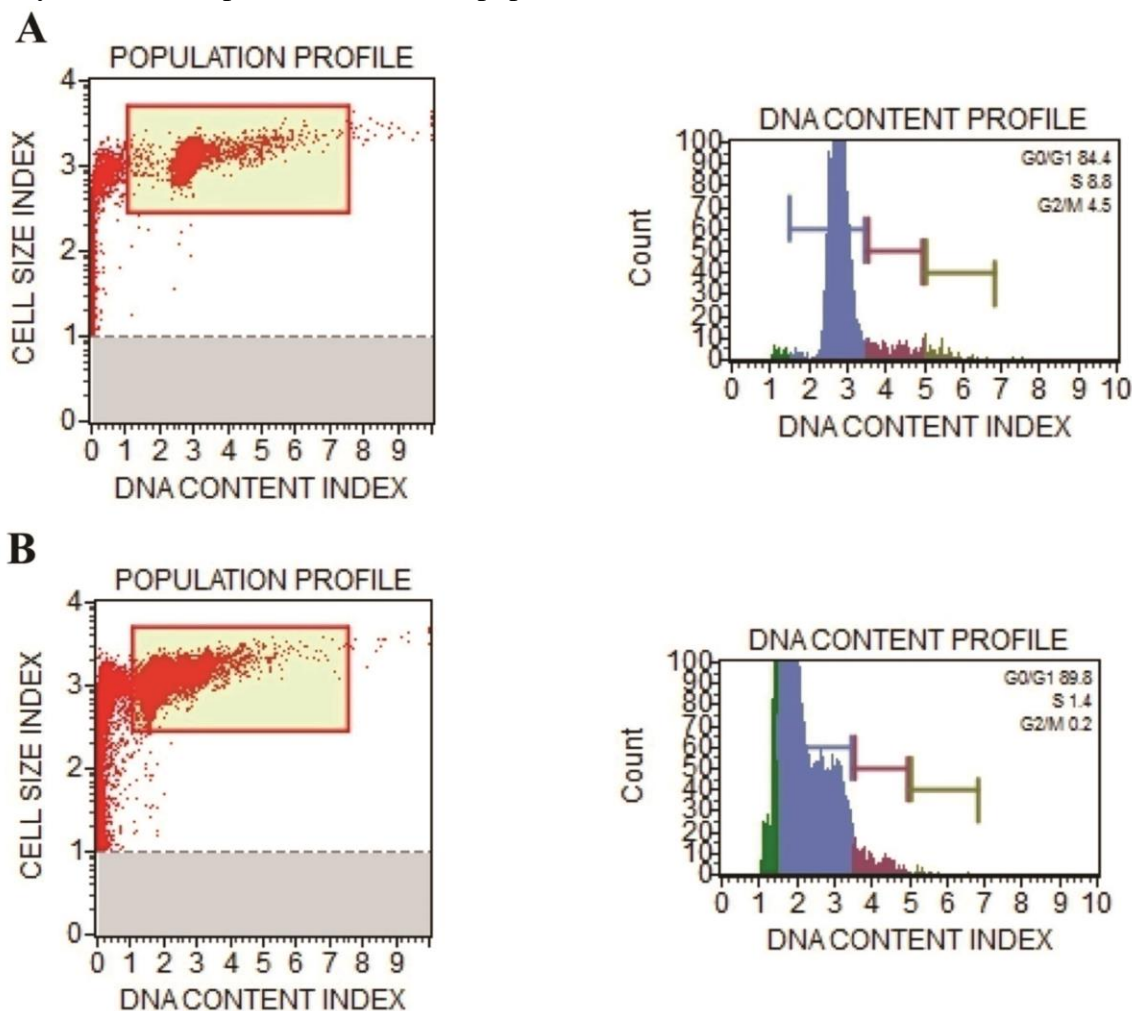


Figure 6. Flow cytometric analysis. (A) untreated A549 cells; (B) HPLC fraction treated A549 cells

3.8. Characterization of bioactive compound.

The collected HPLC bioactive fraction subjected to LCMS/MS analysis showed a retention time of 7.7 in both ionization modes. The m/z values 338 present in both positive and negative ionization was subjected to MS/MS analysis for the determination of elementary composition. The Molecular formula of the compound was $C_{22}H_{44}NO$, and the average mass calculated as 338.34 was shown in Figure 7. From the spectroscopic data, the compound structure was obtained from the ChemSpider database and identified as N-[(3S)-3-[(4R)-2,2-Dimethyltetrahydro-2H-pyran-4-yl]-6-methylheptyl]-4-methylcyclohexanaminium. The functional group of the compound was the tetrahydropyran ring and cyclomethylhexaminium group. The compound consists of functional groups such as cyclohexanaminium derivatives with pyranose ring and demonstrated the broad spectrum of antimicrobial activity of the pyran derivatives [31]. The synthesized novel pyran and furan derivatives have antibacterial and antifungal activities that were reported [32].

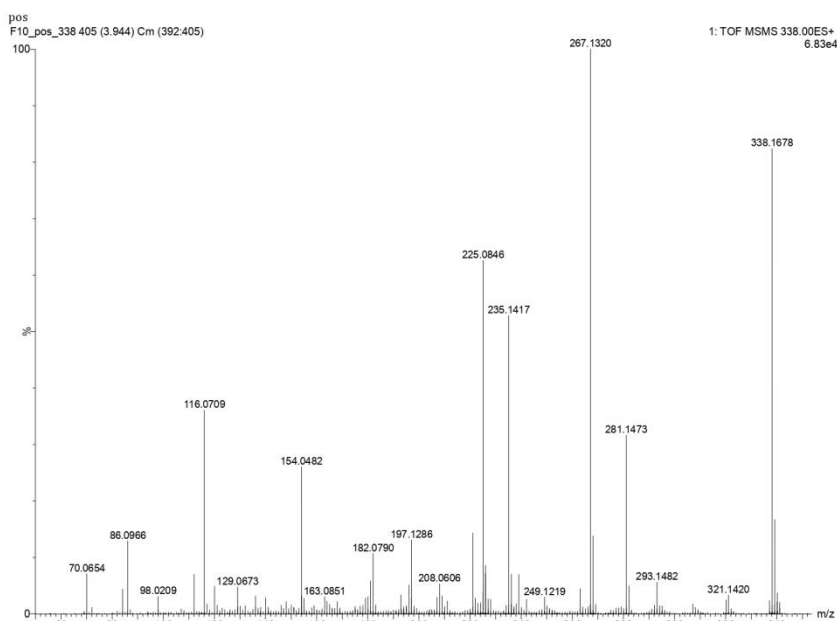


Figure 7. LCMS/MS spectrum. m/z value 338.34.

3.9. Molecular docking.

Molecular docking studies were performed to determine the interaction of N-{(3S)-3-[(4R)-2,2-dimethyl tetrahydro-2H-pyran-4-yl]-6 methyl heptyl} -4-methyl cyclohexanaminium with Bcl-2 and Bcl-XL receptors. The compound had binding energy of -8.62 and -8.24 kcal/mol with anti-apoptotic proteins, Bcl-2 and Bcl-XL, respectively. The compound's tetrahydropyran ring has formed a hydrogen bond with the ARG 68B chain of Bcl-2. The NH₂ group of the cyclohexaminium ring forms a hydrogen bond with GLU 159 and ASN 151 of Bcl-2. The results are shown in Figure 8.

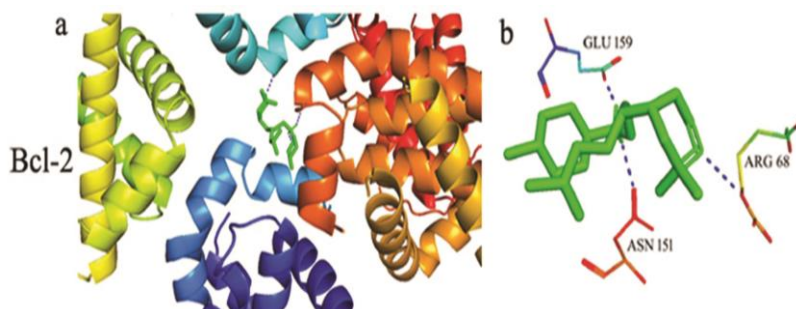


Figure 8. Molecular docking of the compound with anti-apoptotic Bcl-2 protein; (a) Best docking pose of the compound with Bcl-2 protein; (b) Interaction of compound with amino acids.

The compound has shown significant binding interaction with Bcl-XL. The NH₂ of cyclohexanaminium groups showed hydrogen bonding interaction with the Glu 98A chain and Asp 95A chain of anti-apoptotic protein Bcl-XL. The results are shown in Figure 9. The negative value of binding energy indicated the strong binding interaction of the compound with target molecules.

Molecular docking studies using computational methods were used to determine the binding interaction of the purified compounds with the target enzyme [33]. BH3 domains characterize the Bcl-2 family proteins, and that is critical for catalytic activity [34]. The isolated compound binds specifically to the crucial amino acids in the BH3 domain of Bcl-2 and Bcl-XL, resulting in the downstream processing of apoptosis.

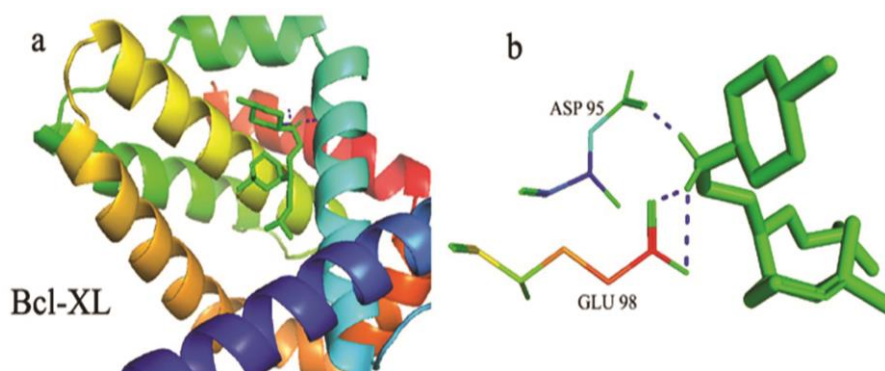


Figure 9. Molecular docking of the compound with anti-apoptotic Bcl-XL protein; (a) Best docking pose of the compound with Bcl-XL protein; (b) Interaction of compound with amino acids.

Moreover, the protein-ligand structures were evaluated for the RMSD, hydrogen bonding, and salt bridge analysis [35]. The results of our study indicated that our compound made strong binding interactions with target proteins, evidenced by having the least binding energy. Based on a molecular docking study, it was inferred that the compound has a significant binding affinity towards the critical amino acids in the BH3 hotspots of anti-apoptotic proteins.

3.9.1. ADMET analysis.

The compound was selected for ADMET analysis and displayed drug-likeness properties, making it suitable for development as an orally active drug. The compound fulfills all the criteria of Lipinski's rule of 5. The drug-likeness and molecular property prediction analysis report is shown in below Table 1.

Table 1. ADMET analysis of the compound.

| Properties | Value |
|-----------------------------------|---------------------------------------|
| Molecular formula | C ₂₂ H ₄₄ NO |
| Molecular weight | 338.34 |
| Number of Hydrogen bond acceptors | 2 |
| Number of Hydrogen bond donors | 1 |
| Freely rotatable bonds | 8 |
| MolLogP | 5.59 |
| MolLog | 5.09 (in Log(moles/L)) 2.76 (in mg/L) |
| MolPSA | 18.75 A ² |
| MolVol | 403.83 A ³ |
| Number of stereo centers | 2 |
| Rule of 5 violations | 1 |

ADMET analysis uses computer simulations to predict the behavior of the compound in the body and can be used in the early stages of drug development [36]. According to the "rule of five," orally active drugs should have a molecular weight under 500 Daltons, limited lipophilicity (expressed by $\log P \leq 5$), a maximum number of 5 hydrogen bond donors, and a maximum number of 10 hydrogen bond acceptors [25]. Molecules violating more than one of these rules are not considered viable drug candidates. The compound of our study strongly followed the Lipinski rule and confirmed that it was soluble and orally active. Hence our study strongly suggested that our compound was a potent inhibitor of anti-apoptotic enzymes and could be used as a potential drug against lung cancer.

The present study proved that the compound identified as tetrahydro pyran derivative of cyclohexaminum group showed *in vitro* anticancer activity against lung cancer (A549) cell lines. The compound showed a cytotoxic effect in A549 cells by activating the mitochondrial apoptotic pathway. Hence the potential compound can be used as a promising chemotherapeutic agent for various cancer treatments. This is the first report on anticancer activity and structure elucidation of the metabolite from *Bacillus aquimaris* KU318396.

4. Conclusions

The marine bacteria MB3 used in the present study were identified as *Bacillus aquimaris*, and the sequence data were submitted to NCBI under the accession number KU318396. Extraction and purification of active anticancer compounds were done using different chromatographic methods such as silica gel column chromatography and HPLC. The molecular characterization was done by LC-MS/MS analysis, and the data revealed the compounds as N-{(3S)-3-[(4R)-2,2-Dimethyltetrahydro-2H-pyran-4-yl]-6 methylheptyl} -4-methyl cyclohexanaminium. The purified compound showed significant cytotoxicity toward lung cancer (A549) cells and most negligible toxicity towards normal L929 (Fibroblast) cells. The apoptotic model of cell death was confirmed by AO/EB staining. The cell cycle analysis revealed the G0/G1 phase arrest and low DNA content at the S phase. The compound showed down-regulation of anti-apoptotic genes and up-regulation of pro-apoptotic genes, suggesting the central downstream signaling of apoptotic pathways. Molecular modeling studies also confirmed the binding potential of the compound with anti-apoptotic target enzymes. Moreover, the ADMET analysis results prove the compound's drug-likeness property. As per the evidence, the present study concludes the anti-lung cancer activity of the bioactive compound from *Bacillus aquimaris*.

Funding

This research was performed with the help of a Mahatma Gandhi University Research Fellowship.

Acknowledgments

This research has no acknowledgment.

Conflicts of Interest

The authors declare no conflict of interest

References

1. Ahmet, T. Sumbul.; Ali, M.; Cengiz, K.; Cemil, B. Akagunduz, B. By 2022 , Cancer Is Now a More Chronic Disease with Chronic Difficulties to Go Along with It. **2022**, *8*, 1–6, <https://doi.org/10.37047/jos.2022-90068>.
2. Noronha, V.; Pinninti, R.; Patil, V.; Joshi, A.; Prabhash, K. Lung Cancer in the Indian Subcontinent. *South Asian J. Cancer* **2016**, *5*, 95, <https://doi.org/10.4103/2278-330x.187571>.
3. Zappa, C.; Mousa, S.A. Non-Small Cell Lung Cancer : *Current Treatment and Future Advances*. **2016**, *5*, 288–300, <https://doi.org/10.21037/tlcr.2016.06.07>.
4. Housman, G.; Byler, S.; Heerboth, S.; Lapinska, K.; Longacre, M.; Snyder, N.; Sarkar, S. Drug Resistance in Cancer: An Overview. *Cancers (Basel)*. **2014**, *6*, 1769–1792, <https://doi.org/10.3390/cancers6031769>.
5. Cotter, T.G. Apoptosis and Cancer: The Genesis of a Research Field. *Nat. Rev. Cancer* **2009**, *9*, 501–507, <https://doi.org/10.1038/nrc2663>.

6. Singh, V.; Khurana, A.; Navik, U.; Allawadhi, P.; Bharani, K.K.; Weiskirchen, R. Apoptosis and Pharmacological Therapies for Targeting Thereof for Cancer Therapeutics. *Sci* **2022**, *4*, 15, <https://doi.org/10.3390/sci4020015>.
7. Verissimo, A.C.S.; Pacheco, M.; Silva, A.M.S.; Pinto, D.C.G.A. Secondary Metabolites from Marine Sources with Potential Use as Leads for Anticancer Applications. *Molecules* **2021**, *26*, 1–13, <https://doi.org/10.3390/molecules26144292>.
8. Hassan, M.; Watari, H.; Abualmaaty, A.; Ohba, Y.; Sakuragi, N. Apoptosis and Molecular Targeting Therapy in Cancer. *Biomed Res. Int.* 2014, *2014*, 150845 <https://doi.org/10.1155/2014/150845>.
9. Karthikeyan, A.; Joseph, A.; Nair, B.G. Promising Bioactive Compounds from the Marine Environment and Their Potential Effects on Various Diseases. *J. Genet. Eng. Biotechnol.* **2022**, *20*, <https://doi.org/10.1186/s43141-021-00290-4>.
10. Paul, S.I.; Majumdar, B.C.; Ehsan, R.; Hasan, M.; Baidya, A.; Bakky, M.A.H.; Stalin, K.; Ravi, L.; Raghavan, V.; Ghosh, S.; et al. Novel Bioactive Compounds From Marine Sources as a Tool for Functional Food Development. *J. Genet. Eng. Biotechnol.* **2022**, *20*, 96–108, <https://doi.org/10.3389/fmars.2022.832957>.
11. Mondol, M.A.M.; Shin, H.J.; Islam, M.T. Diversity of Secondary Metabolites from Marine Bacillus Species: Chemistry and Biological Activity. *Mar. Drugs* **2013**, *11*, 2846–2872, <https://doi.org/10.3390/md11082846>.
12. Ameen, F.; AlNadhari, S.; Al-Homaidan, A.A. Marine Microorganisms as an Untapped Source of Bioactive Compounds. *Saudi J. Biol. Sci.* **2021**, *28*, 224–231, <https://doi.org/10.1016/j.sjbs.2020.09.052>.
13. Weli, A.M.; Ahmed Al-Abd, B.M.; Al-Saidi, A.H.; Aljassasi, H.S.; Hossain, M.A.; Khan, A.; Numan, M.; Al-Jubouri, Y.; Philip, A. The Antibacterial, Antioxidant and Anti Enzymatic Activities of the Leaves' Crude Extracts of Hyoscyamus Gallagheri. *Adv. Biomark. Sci. Technol.* **2022**, *4*, 28–35, <https://doi.org/10.1016/j.abst.2022.06.001>.
14. Shivanand, P.; Jayaraman, G. Isolation and Characterization of a Metal Ion-Dependent Alkaline Protease from a Halotolerant Bacillus Aquimaris VITP4. *Indian J. Biochem. Biophys.* **2011**, *48*, 95–100, <https://pubmed.ncbi.nlm.nih.gov/21682140/>.
15. Atta, H.M.; Radwan, H.G. Biochemical Studies on the Production of Sparsomycin Antibiotic by Pseudomonas Aeruginosa , AZ-SH-B8 Using Plastic Wastes as Fermented Substrate. *J. Saudi Chem. Soc.* **2012**, *16*, 35–44, <https://doi.org/10.1016/j.jscs.2010.10.019>.
16. Patel, S.; Gheewala, N.; Suthar, A.; Shah, A. In-Vitro Cytotoxicity Activity of Solanum Nigrum Extract Against. *Int. J. Pharm. Pharm. Sci.* **2009**, *1*, 38–47, <https://asset-pdf.scinapse.io/prod/2341620185/2341620185.pdf>.
17. Wang, N.; An, J.; Zhang, Z.; Liu, Y.; Fang, J. The Antimicrobial Activity and Characterization of Bioactive Compounds in Peganum Harmala L . Based on HPLC And. *Front. Microbiol.* **2022**, *13*, 1–12, <https://doi.org/10.3389/fmicb.2022.916371>.
18. Raghava Rao, K.V.; Mani, P.; Satyanarayana, B.; Raghava Rao, T. Purification and Structural Elucidation of Three Bioactive Compounds Isolated from Streptomyces Coelicoflavus BC 01 and Their Biological Activity. *3 Biotech* **2017**, *7*, <https://doi.org/10.1007/s13205-016-0581-9>.
19. Alshammari, G.M.; Balakrishnan, A.; Subash-Babu, P.; Al-khalifa, A.; Abdullah Alshatwi, A.; ElGasim Ahmed Yagoub, A.; Naif Al-Harbi, L.; Hamed Alshamlan, G.; Albekairi, N.A. Alpha-Linolenic Acid Rich Allium Porrum Methanolic Extract Potentially Inhibits HT-115 Human Colon Cancer Cells Proliferation via Mitochondria Mediated Apoptotic Mechanism. *J. King Saud Univ. - Sci.* **2022**, *34*, 101736, <https://doi.org/10.1016/j.jksus.2021.101736>.
20. Zeng, C.; Lai, S.; Yao, J.; Zhang, C.; Yin, H.; Li, W. European Journal of Medicinal Chemistry The Induction of Apoptosis in HepG-2 Cells by Ruthenium (II) Complexes through an Intrinsic ROS-Mediated Mitochondrial Dysfunction Pathway. *Eur. J. Med. Chem.* **2016**, *122*, 118–126, <https://doi.org/10.1016/j.ejmech.2016.06.020>.
21. Kennedy, R.K.; Ravindra, V.V.P.; Pragna, N. Phenazine-1-Carboxamide (PCN) from Pseudomonas Sp . Strain PUP6 Selectively Induced Apoptosis in Lung (A549) and Breast (MDA MB-231) Cancer Cells by Inhibition of Antiapoptotic Bcl-2 Family Proteins. *Apoptosis* **2015**, 858–868, <https://doi.org/10.1007/s10495-015-1118-0>.
22. Pumiputavon, K.; Chaowasku, T.; Saenjum, C.; Osathanunkul, M.; Wungsintaweekul, B.; Chawansuntati, K.; Wipasa, J.; Lithanatudom, P. Cell Cycle Arrest and Apoptosis Induction by Methanolic Leaves Extracts of Four Annonaceae Plants. *BMC Complement. Altern. Med.* **2017**, *17*, <https://doi.org/10.1186/s12906-017-1811-3>.
23. Johansson, M.U.; Zoete, V.; Michielin, O.; Guex, N. Defining and Searching for Structural Motifs Using

- DeepView / Swiss-PdbViewer Defining and Searching for Structural Motifs Using DeepView / Swiss-PdbViewer. **2012**, *173*, <https://bmcbioinformatics.biomedcentral.com/articles/10.1186/1471-2105-13-173>.
24. Morris, G.M.; Ruth, H.; Lindstrom, W.; Sanner, M.F.; Belew, R.K.; Goodsell, D.S.; Olson, A.J. Software News and Updates AutoDock4 and AutoDockTools4: Automated Docking with Selective Receptor Flexibility. *J. Comput. Chem.* **2009**, *30*, 2785–2791, <https://doi.org/10.1002/jcc.21256>.
 25. Lipinski, C.A.; Lombardo, F.; Dominy, B.W.; Feeney, P.J. Experimental and Computational Approaches to Estimate Solubility and Permeability in Drug Discovery and Development Settings. *Adv. Drug Deliv. Rev.* **2001**, *46*, 3–26, [https://doi.org/10.1016/s0169-409x\(00\)00129-0](https://doi.org/10.1016/s0169-409x(00)00129-0).
 26. Lalitha, P.; Veena, V.; Vidhyapriya, P.; Lakshmi, P.; Krishna, R.; Sakthivel, N. Anticancer Potential of Pyrrole (1, 2, a) Pyrazine 1, 4, Dione, Hexahydro 3-(2-Methyl Propyl) (PPDHMP) Extracted from a New Marine Bacterium, *Staphylococcus* Sp. Strain MB30. *Apoptosis* **2016**, *5*, 566–577, <https://doi.org/10.1007/s10495-016-1221-x>.
 27. Liu, H.; Wang, H.; Dong, A.; Huo, X.; Wang, H.; Wang, J.; Si, J. The Inhibition of Gastric Cancer Cells' Progression by 23,24-Dihydrocucurbitacin E through Disruption of the Ras/Raf/ERK/MMP9 Signaling Pathway. *Molecules* **2022**, *27*, <https://doi.org/10.3390/molecules27092697>.
 28. Chota, A.; George, B.P.; Abrahamse, H. Interactions of Multidomain Pro-Apoptotic and Anti-Apoptotic Proteins in Cancer Cell Death. *Oncotarget* **2021**, *12*, 1615–1626, <https://doi.org/10.18632/ONCOTARGET.28031>.
 29. Zhou, L.; Chang, D.C. Dynamics and Structure of the Bax-Bak Complex Responsible for Releasing Mitochondrial Proteins during Apoptosis. *J. Cell Sci.* **2008**, *121*, 2186–2196, <https://doi.org/10.1242/jcs.024703>.
 30. Sun, J.; Li, M.; Lin, T.; Wang, D.; Chen, J.; Zhang, Y.; Mu, Q.; Su, H.; Wu, N.; Liu, A.; et al. Cell Cycle Arrest Is an Important Mechanism of Action of Compound Kushen Injection in the Prevention of Colorectal Cancer. *Sci. Rep.* **2022**, *12*, <https://doi.org/10.1038/s41598-022-08336-4>.
 31. Nazari, P.; Bazi, A.; Ayatollahi, S.A.; Dolati, H.; Mahdavi, S.M.; Rafighdoost, L.; Amirmostofian, M. Synthesis and Evaluation of the Antimicrobial Activity of Spiro-4H-Pyran Derivatives on Some Gram Positive and Gram Negative Bacteria. *Iran. J. Pharm. Res.* **2017**, *16*, 943–952, <https://pubmed.ncbi.nlm.nih.gov/29201085/>.
 32. Sarı, E.; Aslan, H.; Dadi, Ş.; Öktemer, A.; Loğoğlu, E. Biological Activity Studies of Some Synthesized Novel Furan and Pyran Derivatives. *J. Sci.* **2017**, *30*, 49–55, <https://dergipark.org.tr/en/pub/gujs/issue/32802/340047>.
 33. Yueniwati, Y.; Syaban, M.F.R.; Faratisha, I.F.D.; Yunita, K.C.; Kurniawan, D.B.; Putra, G.F.A.; Erwan, N.E. Molecular Docking Approach of Natural Compound from Herbal Medicine in Java against Severe Acute Respiratory Syndrome Coronavirus-2 Receptor. *Open Access Maced. J. Med. Sci.* **2021**, *9*, 1181–1186, <https://doi.org/10.3889/oamjms.2021.6963>.
 34. Moroy, G.; Martin, E.; Dejaegere, A.; Stote, R.H. Molecular Basis for Bcl-2 Homology 3 Domain Recognition in the Bcl-2 Protein Family: Identification of Conserved Hot Spot Interactions. *J. Biol. Chem.* **2009**, *284*, 17499–17511, <https://doi.org/10.1074/jbc.M805542200>.
 35. Mei, X.; Li, X.; Zhao, C.; Liu, A.; Ding, Y.; Shen, C.; Li, J. The Use of Molecular Dynamics Simulation Method to Quantitatively Evaluate the Affinity between HBV Antigen T Cell Epitope Peptides and HLA-A Molecules. *Int. J. Mol. Sci.* **2022**, *23*, <https://doi.org/10.3390/ijms23094629>.
 36. Saida, K.; Salah, B.; Mohamed, B.; Samir, C.; Md Amiruddin, H.; F.A.Q. QSAR Modeling , Molecular Docking , ADMET Prediction and Molecular Dynamics Simulations of Some 6-Arylquinazolin-4-Amine Derivatives as DYRK1A Inhibitors . *J. Mol. Struct.* **2022**, *1258*, 132659, <https://doi.org/10.1016/j.molstruc.2022.132659>.